International Journal of
Mathematical Modelling & Computations
Vol. 14, No. 03, Summer 2024, 231- 240
DOI:10.71932/ijm.2024.1196293

Numerical solution of the spread model of COVID-19 by using Müntz functions

Afkar Kareem Mnahi[a], Majid Tavassoli Kajani[a,*]

Mohammed Jasim Mohammed[b], Masoud Allame[a]

[a] *Department of Mathematics, Isfahan(Khorasgan) Branch, Islamic Azad University, Isfahan, Iran*;
[b] *Department of Mathematics, University of Thi-Qar, Nasiriyah, 64001, Iraq.*

Abstract. The outbreak of COVID-19 has necessitated the development of various mathematical models to understand and predict its spread. Among these, fractional differential equations have gained attention for their ability to capture the complexity and dynamics of infectious disease transmission. However, obtaining analytical solutions for such models is often infeasible. In this paper, we present an approach to approximate solutions of a fractional differential equation that describes the spread of COVID-19. The fractional order in the model reflects the memory and hereditary properties of the disease transmission process, which are not adequately described by traditional integer-order models. To tackle the complexities of this equation, we utilize Müntz functions, which are a class of basis functions used in approximation theory. Müntz functions are particularly useful due to their flexible nature and ability to converge to various types of functions, making them suitable for approximating solutions to differential equations. We perform numerical simulations to evaluate the performance of the Müntz functions in approximating the solution of our model. The findings indicate that the Müntz function approach yields superior accuracy in modeling the spread of COVID-19 compared to these alternative methods.

Received: 06 April 2024, Revised: 24 August 2024, Accepted: 25 September 2024.

Keywords: Müntz function; Fractional Differential Equations; Collocation Method; Spread model of COVID-19.

AMS Subject Classification: 65Txx, 65Z05, 34A08.

Index to information contained in this paper

*Corresponding author. Email: tavassoli_k@yahoo.com, mtavassoli@khuisf.ac.ir

1. Introduction

One of the viruses that led to the deaths of millions worldwide was the SARS-CoV-2, the virus responsible for COVID-19. Emerging in late 2019, it quickly escalated into a global pandemic, presenting unprecedented challenges to public health systems and societies. In the early stages of the outbreak, governments around the world implemented various measures to control and reduce the transmission of the virus. These strategies included social distancing, travel restrictions, and encouraging personal hygiene practices, all aimed at minimizing infection rates.

Several factors contributed to the spread of COVID-19, including close interactions between infected and healthy individuals within communities, human mobility, and socio-economic conditions that influenced behavior. Notably, crowded settings and insufficient public health infrastructure heightened the risk of viral transmission. Consequently, authorities enforced movement restrictions and initiated quarantines in affected areas to reduce contamination levels and slow the rate of infection. These public health measures were crucial in managing the early phases of the pandemic and preventing healthcare systems from becoming overwhelmed [1–4].

Simultaneously, scientists and researchers developed numerous mathematical models to analyze the dynamics of COVID-19 spread. These models aimed to capture the complex interactions among variables such as infection rates, recovery rates, and population densities. However, finding analytical solutions to these models often proved challenging or impossible due to the nonlinear nature of the governing equations [5–14]. This complexity arises from the need to account for real-world variables, including varying transmission rates, asymptomatic cases, and the effects of public health interventions.

Given these challenges, researchers have turned to various numerical methods to derive approximate solutions. These methods, which include finite difference methods, agent-based models, and computational simulations, serve to provide insights into the potential trajectories of the virus and the effectiveness of different intervention strategies. Among these approaches, the use of Müntz functions has garnered attention as a promising tool for modeling complex phenomena due to their ability to represent a wide range of functions with varying smoothness.

In this article, we seek to derive an approximate solution for the COVID-19 diffusion model utilizing Müntz functions and Müntz collocation points. This approach not only offers a flexible framework for approximating solutions to the differential equations governing the spread of the virus but also deepens our understanding of the underlying dynamics. By employing this methodology, we aim to provide valuable insights that can assist policymakers and public health officials in their ongoing response to the pandemic, ultimately striving to enhance strategies to curb the virus's spread and safeguard public health.

2. Initial definitions

2.1 *Derivative and fractional integral*

Definition 2.1 The Riemann-Liouville fractional integral operator for the function $f \in L^2[0,1]$ and $\alpha \in \mathbb{R}^+$ is defined as follows [15]:

$$\mathcal{I}^{\alpha} f(t) = \frac{1}{\Gamma(\alpha)} \int_0^t \frac{f(\tau)}{(t-\tau)^{1-\alpha}} d\tau. \tag{1}$$

Definition 2.2 The Caputo fractional derivative operator for the function $f \in L^2[0,1]$, where $n-1 < \alpha \leqslant n$, $n \in \mathbb{N}$ is defined as follows [15]:

$$\mathcal{D}^{\alpha} f(t) = \frac{1}{\Gamma(n-\alpha)} \int_0^t \frac{f^{(n)}(\tau)}{(t-\tau)^{\alpha+1-n}} d\tau. \tag{2}$$

For $\alpha \in \mathbb{R}^+$ and $n \in \mathbb{N}$, we have:

$$\mathcal{I}^{\alpha}(\mathcal{D}^{\alpha} f(t)) = f(t) - \sum_{k=0}^{n-1} f^k(0) \frac{t^k}{k!},$$

$$\mathcal{D}^{\alpha} f(t) = I^{n-\alpha}(\mathcal{D}^n f(t)) \ , \ n-1 < \alpha \leqslant n.$$

2.2 *Properties of Müntz orthogonal functions*

Definition 2.3 The family $\{p_n(t)\}_{n=0}^{\infty}$ represents a class of Müntz orthogonal functions that are orthogonal on the interval $[0,1]$ with respect to the weight function $w(t) = 1$. These Müntz functions are defined as follows [16]:

$$p_n(t) = \mathcal{R}_n(t) + \mathcal{S}_n(t) \ln(t), \ n = 0, 1, 2, \ldots, \ t \in [0,1],$$

in which $\mathcal{R}_n(t)$ and $\mathcal{S}_n(t)$ are polynomials of order $\left[\frac{n}{2}\right]$ and $\left[\frac{n-1}{2}\right]$ respectively, then is:

$$\mathcal{R}_n(t) = \sum_{v=0}^{[\frac{n}{2}]} a_v^{(n)} t^v \ , \ \mathcal{S}_n(t) = \sum_{v=0}^{[\frac{n-1}{2}]} b_v^{(n)} t^v$$

for $n = 2m$ and $0 \leqslant v \leqslant m-1$, the explicit expression for the coefficients is given by:

$$a_v^{(2m)} = -\begin{pmatrix} m+v \\ m \end{pmatrix}^2 \begin{pmatrix} m \\ v \end{pmatrix}^2 \left[\frac{2m+1}{2v+1} + 2(m-v) \sum_{j=0, j\neq v}^{m-1} \frac{2j+1}{(j-v)(j+v+1}} \right],$$

and

$$b_v^{(2m)} = -(m-v) \begin{pmatrix} m+v \\ m \end{pmatrix}^2 \begin{pmatrix} m \\ v \end{pmatrix}^2,$$

and for $v = m$

$$a_v^{(2m)} = \begin{pmatrix} 2m \\ m \end{pmatrix}^2 \ , \ b_v^{(2m)} = 0.$$

for $n = 2m+1$ and $0 \leqslant v \leqslant m$, we have the following explicit expression for the coefficients:

$$a_v^{(2m)} = \begin{pmatrix} m+v \\ m \end{pmatrix}^2 \begin{pmatrix} m \\ v \end{pmatrix}^2 \left[\frac{2m+1}{2v+1} + 2(m+v+1) \sum_{j=0, j\neq v}^{m-1} \frac{2j+1}{(j-v)(j+v+1}} \right],$$

Table 1. The roots of p_{10}.

i	t_i (roots of p_{10})
1	0.248244164962838089008215036157594l4e-3
2	0.484373444377592286864145720922210l2e-2
3	0.264018954880526063563729211185634l0e-1
4	0.814257045396240446227036719493827l7e-1
5	0.182642982492702492509204828108067l5
6	0.331650431261879891684772180471539l7
7	0.515143567891989884791214916136966l5
8	0.706143634432712118373837955142270l7
9	0.870118903125375899514621752734009l1
10	0.974181833786116399172392777524870l9

and

$$b_v^{(2m)} = (m+v+1)\begin{pmatrix} m+v \\ m \end{pmatrix}^2 \begin{pmatrix} m \\ v \end{pmatrix}^2.$$

Orthogonal functions of Müntz can be identified using the following approach

$$p_0(t) = 1,$$

$$p_1(t) = 1 + \ln(t),$$

$$p_2(t) = -3 + 4t - \ln(t),$$

$$p_3(t) = 9 - 8t + 2(1+6t)\ln(t),$$

$$p_4(t) = -11 - 24t + 36t^2 - 2(1+18t)\ln(t).$$

Theorem 2.1 The function $p_n(t)$ on the interval $[0,1]$ has exactly n distinct simple roots [16].

For example, the roots of p_{10} are given in Tables 1.

Theorem 2.2 Müntz functions are orthogonal and satisfy the following relation [16]:

$$\int_0^1 p_i(t)p_j(t)dt = \begin{cases} \frac{1}{\delta_j}, \, i = j, \\ \\ 0, \; i \neq j, \end{cases}$$

in which

$$\delta_j = \begin{cases} j+1, \, j \text{ even}, \\ \\ j, \quad j \text{ odd}, \end{cases}$$

2.3 *Approximation by Müntz function*

Assume that $f \in L^2[0,1]$. We approximate the function f using a linear combination of Müntz functions:

$$f(t) \simeq \widetilde{f}(t) = \sum_{i=0}^{n} c_i p_i(t). \tag{3}$$

Now, based on the relation (3), the unknown coefficients c_i are determined through the following approach:

$$c_i = \frac{1}{\delta_j} \int_0^1 f(t)p_i(t)dt, \quad i = 0, 1, 2, \ldots, n.$$

Theorem 2.3 Suppose that $f \in H^r(0,1)$ with integers $r \geqslant 0$ where [17, 18]

$$H^r(a,b) = \{v \in \mathbb{C}^{r-1}([a,b]) : \frac{d}{dx}v^{r-1} \in L^2(a,b)\},$$

is the Sobolev space. Let $\widetilde{f}(t) = \sum_{i=0}^{n} c_i p_i(t)$ be the best approximation of f in $span\{p_0(t), p_1(t), ..., p_n(t)\}$. Then, if $r \leqslant n+1$ we have

$$\|f - \widetilde{f}\|_{L^2(0,1)} \leqslant c(n+1)^{-r}\|f^{(r)}\|_{L^2(0,1)},$$

and for $1 \leqslant \mu \leqslant r$ we have

$$\|f - \widetilde{f}\|_{H^\mu(0,1)} \leqslant c(n+1)^{2\mu-\frac{1}{2}-r}\|f^{(r)}\|_{L^2(0,1)},$$

where c is a constant depending only on r.

3. Numerical solution of the spread model of COVID-19

We consider a fractional SEIR model for the spread of the corona virus in [19] and we solve this model by Caputo's fractional derivative. The data of the model is based on the data presented in [19]. In general, we consider the fractional differential equations as follows

$$\begin{cases} \mathcal{D}^{\alpha_1} S(t) = \Lambda - (\lambda + ae + \mu)S(t), \\ \mathcal{D}^{\alpha_2} E(t) = aeS(t) + (\theta + \mu + (1-\eta)\lambda)E(t), \\ \mathcal{D}^{\alpha_3} I(t) = \lambda S(t) + (1-\eta)E(t) - (\mu + \delta + \gamma)I(t), \\ \mathcal{D}^{\alpha_4} R(t) = \theta E(t) + \gamma I(t) - \mu R(t). \end{cases} \tag{4}$$

Considering the initial conditions for the system of equation mentioned above:

$$S(0) = S_0, \quad E(0) = E_0, \quad I(0) = I_0, \quad R(0) = R_0.$$

Where $\mathcal{D}^{\alpha_i}$, $i = 1, 2, 3, 4$ represents Caputo's fractional derivative operator of order $0 < \alpha_i \leqslant 1$.

Approximating the left hand side of Eq. (4) by a linear combination of the Müntz

functions on the interval $[0,1]$, we have:

$$\begin{cases} \mathcal{D}^{\alpha_1} S(t) = \sum_{i=0}^{n} c_i^S p_i(t), \\ \mathcal{D}^{\alpha_2} E(t) = \sum_{i=0}^{n} c_i^E p_i(t), \\ \mathcal{D}^{\alpha_3} I(t) = \sum_{i=0}^{n} c_i^I p_i(t), \\ \mathcal{D}^{\alpha_4} R(t) = \sum_{i=0}^{n} c_i^R p_i(t), \end{cases}$$

where c_i^S, c_i^E, c_i^I and c_i^R are the unknown coefficients that have to be found.

To obtain an approximation of the functions $S(t), E(t), I(t)$ and $R(t)$, we apply the Riemann-Liouville fractional to both sides of the above:

$$\begin{cases} S(t) = \mathcal{I}^{\alpha_1} \sum_{i=0}^{n} c_i^S p_i(t) + S_0, \\ E(t) = \mathcal{I}^{\alpha_2} \sum_{i=0}^{n} c_i^E p_i(t) + E_0, \\ I(t) = \mathcal{I}^{\alpha_3} \sum_{i=0}^{n} c_i^I p_i(t) + I_0, \\ R(t) = \mathcal{I}^{\alpha_4} \sum_{i=0}^{n} c_i^R p_i(t) + R_0. \end{cases} \tag{5}$$

In this way, the relation (4) can be rewritten as follows

$$\begin{cases} \sum_{i=0}^{n} c_i^S p_i(t) = \Lambda - (\lambda + ae + \mu) \left(\mathcal{I}^{\alpha_1} \sum_{i=0}^{n} c_i^S p_i(t) + S_0 \right), \\ \sum_{i=0}^{n} c_i^E p_i(t) = ae \left(\mathcal{I}^{\alpha_1} \sum_{i=0}^{n} c_i^S p_i(t) + S_0 \right) + (\theta + \mu + (1-\eta)\lambda) \left(\mathcal{I}^{\alpha_2} \sum_{i=0}^{n} c_i^E p_i(t) + E_0 \right), \\ \sum_{i=0}^{n} c_i^I p_i(t) = \lambda \left(\mathcal{I}^{\alpha_1} \sum_{i=0}^{n} c_i^S p_i(t) + S_0 \right) + (1-\eta) \left(\mathcal{I}^{\alpha_2} \sum_{i=0}^{n} c_i^E p_i(t) + E_0 \right) - (\mu + \delta + \gamma) \left(\mathcal{I}^{\alpha_3} \sum_{i=0}^{n} c_i^I p_i(t) + I_0 \right), \\ \sum_{i=0}^{n} c_i^R p_i(t) = \theta \left(\mathcal{I}^{\alpha_2} \sum_{i=0}^{n} c_i^E p_i(t) + E_0 \right) + \gamma \left(\mathcal{I}^{\alpha_3} \sum_{i=0}^{n} c_i^I p_i(t) + I_0 \right) - \mu \left(\mathcal{I}^{\alpha_4} \sum_{i=0}^{n} c_i^R p_i(t) + R_0 \right). \end{cases} \tag{6}$$

By substituting t_i, the roots of $p_{n+1}(x)$, into the relation (6), we obtain:

$$\begin{cases} \sum_{i=0}^{n} c_i^S p_i(t_i) = \Lambda - (\lambda + ae + \mu) \left(\mathcal{I}^{\alpha_1} \sum_{i=0}^{n} c_i^S p_i(t_i) + S_0 \right), \\ \sum_{i=0}^{n} c_i^E p_i(t_i) = ae \left(\mathcal{I}^{\alpha_1} \sum_{i=0}^{n} c_i^S p_i(t_i) + S_0 \right) + (\theta + \mu + (1-\eta)\lambda) \left(\mathcal{I}^{\alpha_2} \sum_{i=0}^{n} c_i^E p_i(t_i) + E_0 \right), \\ \sum_{i=0}^{n} c_i^I p_i(t_i) = \lambda \left(\mathcal{I}^{\alpha_1} \sum_{i=0}^{n} c_i^S p_i(t_i) + S_0 \right) + (1-\eta) \left(\mathcal{I}^{\alpha_2} \sum_{i=0}^{n} c_i^E p_i(t_i) + E_0 \right) - (\mu + \delta + \gamma) \left(\mathcal{I}^{\alpha_3} \sum_{i=0}^{n} c_i^I p_i(t_i) + I_0 \right), \\ \sum_{i=0}^{n} c_i^R p_i(t_i) = \theta \left(\mathcal{I}^{\alpha_2} \sum_{i=0}^{n} c_i^E p_i(t_i) + E_0 \right) + \gamma \left(\mathcal{I}^{\alpha_3} \sum_{i=0}^{n} c_i^I p_i(t_i) + I_0 \right) - \mu \left(\mathcal{I}^{\alpha_4} \sum_{i=0}^{n} c_i^R p_i(t_i) + R_0 \right). \end{cases} \tag{7}$$

As a result, Eq. (7) generates a system of $4(n+1)$ with $4(n+1)$ coefficients. By solving this system using one of the existing methods the unknown coefficients c_i^S, c_i^E, c_i^I and c_i^R will be determined, and the approximations of the functions

Table 2. The values of $S(t)$ using the presented method for $N = 15$ and different values of t and α.

t	$\alpha = 0.75$	$\alpha = 0.85$	$\alpha = 0.90$	$\alpha = 0.98$
0	220.892	220.892	220.892	220.892
0.2	172.2441727	178.9846394	182.1934960	187.0399057
0.4	146.4785388	151.7687723	154.5602979	159.1638510
0.6	128.0058666	130.9230381	132.6451029	135.7568293
0.8	113.751266	114.2471624	114.7631771	115.9943740
1	102.27040	100.580912	99.940580	99.2580837

Table 3. The values of $E(t)$ using the presented method for $N = 15$ and different values of t and α.

t	$\alpha = 0.75$	$\alpha = 0.85$	$\alpha = 0.90$	$\alpha = 0.98$
0	220.818	220.818	220.818	220.818
0.2	215.1945311	216.1321585	216.5515655	217.1574898
0.4	211.4024731	212.4162192	212.9028341	213.6484348
0.6	208.1535134	209.0477473	209.5016541	210.2295847
0.8	205.2268525	205.9025113	206.2688095	206.8862303
1	202.524186	202.9238940	203.1674338	203.6111049

Table 4. The values of $I(t)$ using the presented method for $N = 15$ and different values of t and α.

t	$\alpha = 0.75$	$\alpha = 0.85$	$\alpha = 0.90$	$\alpha = 0.98$
0	0.0320	0.0320	0.0320	0.0320
0.2	0.1048955168	0.09423694162	0.08925608237	0.08182975944
0.4	0.1463247043	0.1370191586	0.1322677080	0.1246230086
0.6	0.1777841789	0.1715579864	0.1681154634	0.1621929072
0.8	0.203398175	0.2006651572	0.1988844867	0.1954550789
1	0.22508840	0.225791490	0.225746641	0.2250818840

Table 5. The values of $R(t)$ using the presented method for $N = 15$ and different values of t and α.

t	$\alpha = 0.75$	$\alpha = 0.85$	$\alpha = 0.90$	$\alpha = 0.98$
0	0.00855	0.00855	0.00855	0.00855
0.2	0.05236691334	0.04521784215	0.04199530633	0.03731458397
0.4	0.08104211218	0.07359737873	0.06998115135	0.06439086309
0.6	0.1050462374	0.09878560971	0.09555292898	0.09029996099
0.8	0.126220057	0.1218405623	0.1193956130	0.1151844982
1	0.145396619	0.143259020	0.141841409	0.1391241700

$S(t), E(t), I(t)$ and $R(t)$ over the interval $[0, 1]$ will be obtained.

4. Numerical results

The parameters of the model (4) are as follows:

$$\Lambda = 0.080, \quad a = 0.000761, \quad \mu = 0.080$$
$$\lambda = 0.00073, \quad \delta = 0.00039, \quad e = 1$$
$$\theta = 0.00064, \quad \eta = 0.3998, \quad \gamma = 0.000326$$
$$S(0) = 220.892, \quad E(0) = 220.818, \quad I(0) = 0.0320, \quad R(0) = 0.00855$$

In this example, we assume that $\alpha_1 = \alpha_2 = \alpha_3 = \alpha_4 = \alpha$, and present the numerical results of the proposed method. Figures 1-4 respectively show graphes of $S(t)$, $E(t)$, $I(t)$ and $R(t)$ for $N = 10$ and different values of α. In addition, Tables 2-5 respectively display the values of $S(t)$, $E(t)$, $I(t)$ and $R(t)$ obtained with the presented method for $N = 15$ and different values of α.

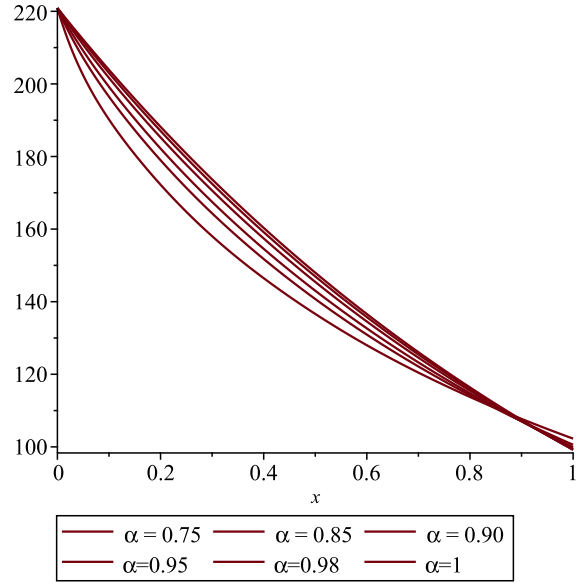

Figure 1. Graph $S(t)$ using the presented method for $N = 10$ and different values of α.

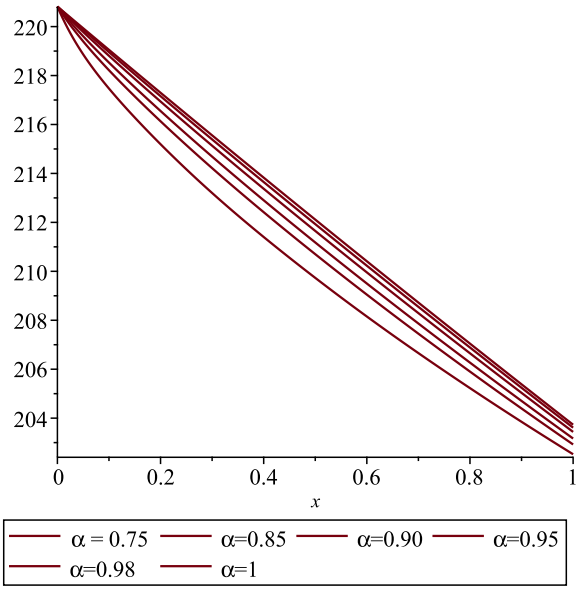

Figure 2. Graph $E(t)$ using the presented method for $N = 10$ and different values of α.

5. Conclusion

The Müntz orthogonal functions exhibit distinct roots within the interval [0, 1], which serve as valuable collocation points in numerical analysis. Utilizing these collocation points, we have successfully implemented a model to analyze the spread of COVID-19. The outcomes of this modeling approach reveal not only the robustness of the Müntz orthogonal functions in capturing the dynamics of the virus but also their capability to provide accurate and reliable results. The numerical findings underscore the efficiency of this method, demonstrating its effectiveness in addressing complex models. This approach not only enhances the understanding of

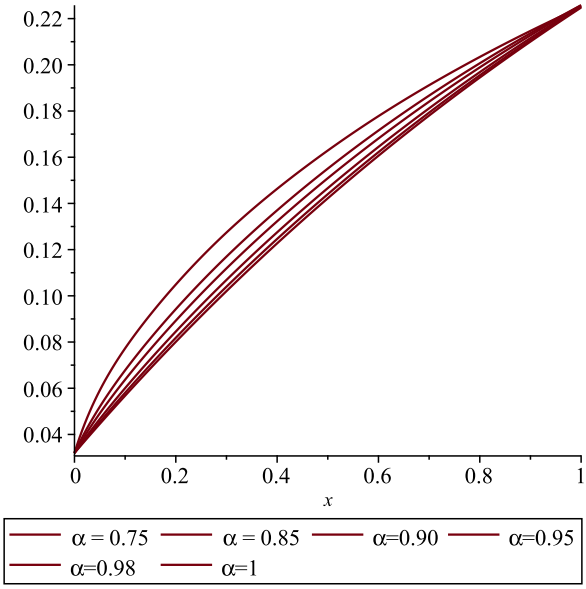

Figure 3. Graph $I(t)$ using the presented method for $N = 10$ and different values of α.

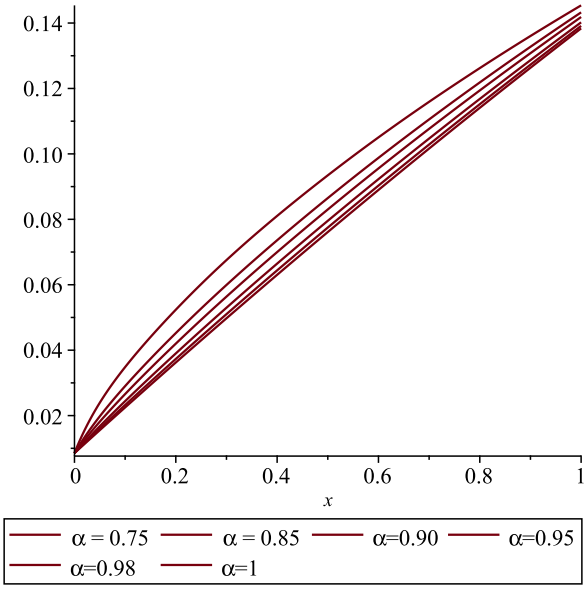

Figure 4. Graph $R(t)$ using the presented method for $N = 10$ and different values of α.

the COVID-19 trajectory but also paves the way for further applications in various fields requiring similar analytical techniques. Future research could explore extending this methodology to incorporate varying parameters or applying it to different epidemiological models, creating opportunities for deeper insights and potential advancements in public health strategies.

References

[1] M. Goyal, H.M. Baskonus and A. Prakash, An efficient technique for a time fractional model of lassa hemorrhagic fever spreading in pregnant women, Eur. Phys. J. Plus, **134**(481) (2019) 1-10.

[2] W. Gao, P. Veeresha, D.G. Prakasha, H.M. Baskonus and G. Yel, New approach for the model describing the deathly disease in pregnant women using Mittag-Leffler function, Chaos, Solitons Fract, **134** (2020), Article 109696.
[3] D. Kumar, J. Singh, M. Al-Qurashi and D. Baleanu, A new fractional SIRS-SI malaria disease model with application of vaccines, anti-malarial drugs, and spraying, Adv. Diff. Eq., **278** (2019) 1-10.
[4] K. Shah, M.A. Alqudah, F. Jarad and T. Abdeljawad, Semi-analytical study of pine wilt disease model with convex rate under Caputo-Febrizio fractional order derivative, Chaos, Solitons Fract, **135** (2020), Article 109754.
[5] M.R. Gandomani and M. Tavassoli Kajani, Numerical solution of a fractional order model of HIV infection of CD4 + T cells using Müntz-Legendre polynomials, International Journal Bioautomation, **20**(2) (2016) 193-204.
[6] X. Tian, C. Li, A. Huang, S. Xia, S. Lu, Z. Shi, L. Lu, S. Jiang, Z. Yang, Y. Wu and T. Ying, Potent binding of 2019 novel coronavirus spike protein by a SARS coronavirus-specific human monoclonal antibody, Emerg Microbes Infect, **9**(1) (2020) 382-385.
[7] J.F.W. Chan, K.H. Kok, Z. Zhu, H. Chu, K.K.W. To, S. Yuan and K.Y. Yuen, Genomic characterization of the 2019 novel human-pathogenic coronavirus isolated from a patient with atypical pneumonia after visiting Wuhan, Emerg Microbes Infect, **9**(1) (2020) 221-236.
[8] K. Shah, M. Arfan, I. Mahariq, A. Ahmadian, S. Salahshour and M. Ferrara, Fractal-fractional mathematical model addressing the situation of corona virus in Pakistan, Result Phys., **19** (2020), Article 103560.
[9] M. Bahmanpour, M. Tavassoli-Kajani and M. Maleki, A Müntz wavelets collocation method for solving fractional differential equations, Computational and Applied Mathematics, **37**(4) (2018) 5514-5526.
[10] M. Maleki and M. Tavassoli Kajani, Numerical approximations for Volterra's population growth model with fractional order via a multi-domain pseudospectral method, Applied Mathematical Modelling, **39** (2015),4300-4308.
[11] M. Tavassoli Kajani, Numerical solution of fractional pantograph equations via Müntz-Legendre polynomials, Mathematical science, **18**(3) (2024) 387-395.
[12] D. Shirani, M. Tavassoli Kajani and S. Salahshour , Numerical Solution of a SIR Fractional Model of the Distribution of Computer Viruses Using Dickson Polynomials, Int. J. Industrial Mathematics , **13**(3), (2021) 323-331.
[13] M.R. Gandomani and M. Tavassoli Kajani, Numerical Solution of a Fractional Order Model of HIV Infection of CD4$^+$T Cells Using Müntz-Legendre Polynomials, INT. J . BIO AUTOMATION, **20**(2) (2016), 193-204.
[14] M.R. Gandomani and M. Tavassoli Kajani, Application of shifted Müntz-Legender Polynomials for solving fractional differential equations, International Journal of Pure and Applied Mathematics, **103**(2) (2015), 263-279.
[15] A. Saadatmandi and S. Akhlaghi, Using hybrid of Block-Pulse functions and Bernoulli polynomials to solve fractional Fredholm-Volterra integro-differential equations, Sains Malaysiana, **49**(4) (2020), 953-962.
[16] G.V. Milovanović, Müntz orthogonal polynomials and their numerical evaluation, Applications and Computation of Orthogonal Polynomials, Springer, Oberwolfach Germany, 1998, 179-194.
[17] C. Canuto, M. Y. Hussaini, A. Quarteroni and T.A. Zang, Spectral Methods. Fundamentals in Single Domains, Springer, Berlin Heidelberg New York (2006).
[18] S. Akhlaghi, M. Tavassoli Kajani and M. Allame, Numerical Solution of Fractional Order Integro-Differential Equations via Müntz Orthogonal Functions, Journal of Mathematics, 2023, 6647128, 1-13.
[19] Muhammad Arfan, Hussam Alrabaiah, Mati Ur Rahman, Yu-Liang Sun, Ahmad Sobri Hashim, Bruno A. Pansera, A. Ahmadian and S. Salahshour, Investigation of fractal-fractional order model of COVID-19 in Pakistan under Atangana-Baleanu Caputo (ABC) derivative, Results in Physics, **24** (2021),104046.